American Industrial Hygiene Association Journal

ISSN: 0002-8894 (Print) (Online) Journal homepage: https://www.tandfonline.com/loi/aiha20

COMPUTATION OF THE INITIALLY UNKNOWN BOUNDARIES OF FLOW FIELDS GENERATED BY LOCAL EXHAUST HOODS

Mazen Y. Anastas

To cite this article: Mazen Y. Anastas (1991) COMPUTATION OF THE INITIALLY UNKNOWN BOUNDARIES OF FLOW FIELDS GENERATED BY LOCAL EXHAUST HOODS, American Industrial Hygiene Association Journal, 52:9, 379-386, DOI: 10.1080/15298669191364901

To link to this article: https://doi.org/10.1080/15298669191364901

COMPUTATION OF THE INITIALLY UNKNOWN BOUNDARIES OF FLOW FIELDS GENERATED BY LOCAL EXHAUST HOODS*

Mazen Y. Anastas

National Institute for Occupational Safety and Health, 4676 Columbia Parkway, Cincinnati, OH 45226

Local exhaust hoods are important in controlling contaminants in the workplace. To predict hood effectiveness, it is important to have knowledge of the airflow field that it generates. Currently, there are theoretical models adequate for predicting the flow fields of hoods with flanged openings. These models are solutions of Laplace's equation in terms of the velocity potential. Comparison of experimental and theoretical values of air velocities show good agreement. With the exception of the plain slot, no such models are available for plain hoods or other hoods with complex geometries. This paper explores the feasibility of approximating the equal air velocity contours for any local exhaust hood by assuming that these contours are also equipotential contours. A slot configuration, for which an analytical model is available, was used to evaluate the accuracy of the assumption. Starting with a good approximation for the 15% velocity contour, three other boundaries were generated. The procedure used in generating boundaries after the initial one involved solution of Laplace's equation, assuming constant potential along the boundary and adjustment of boundary location on the basis of differences between the calculated value of the normal derivative of the velocity potential at a point on the boundary and the specified value (15%). The next-to-last boundary generated by the procedure exhibited an oscillation in the values of the normal derivative, which was detrimental to the desired solution. Possible causes for this oscillation and possible refinements in the procedure are discussed.

Local exhaust devices are commonly used to capture contaminants generated by many industrial processes before these contaminants become dispersed in the workplace and cause employee overexposures. The geometries and suction rates of these devices are dictated by many factors, including process geometry and contaminant generation characteristics. The latter would include the rate and velocity at which contaminants are generated and phase (gas, liquid, or solid). Prior knowledge of airflow patterns is very important in predicting an exhaust hood's ability to capture contaminants. Heinsohn and Choi[1] demonstrated the usefulness of airflow patterns in predicting capture characteristics of exhaust hoods for flanged and unflanged slots with respect to particulate matter. Slots are rectangular openings of aspect ratio (AR) approaching zero (AR is the ratio of width to length of a rectangle).

Early research by Dalla Valle[2] and by Silverman,[3,4] aimed at predicting the airflow patterns produced by local exhaust hoods, involved the development of empirical centerline velocity models for flanged and plain basic openings (circle and rectangle). These empirical models are reported in the American Conference of Governmental Industrial Hygienists' *Industrial Ventilation—A Manual of Recommended Practice*.[5] More recently, Anastas and Hughes[6] used potential flow theory to derive centerline velocity models for flanged hoods. They found excellent agreement between theoretical and experimental centerline data. They also found that the theoretical model for rectangular hoods provided identical centerline velocities to those provided by a model for slots (AR = 0) at AR = 0.01 or less.

Centerline models can predict the capture characteristics of a hood along the centerline only. Of course, this is not sufficient to define the capture characteristics of a hood in the space in which it is located. The first airflow modeling effort for hoods that generate three-dimensional (3-D) equal velocity contours was performed by Tyaglo and Shepelev[7] for infinitely flanged rectangles. They derived equations for the components of air velocity that were related to the average velocity through the face and the values of the coordinates at a point in space, and these equations applied to the full range of AR (0 to 1). The model was derived by assuming that the face of the hood is divided into many area sinks, each of which contributes to the level of the velocity potential at a point in space. The validity of the model was verified experimentally by using a rectangular hood of AR = 0.1. The authors reported "agreement" between experimental and theoretical centerline velocities.

Drkal[8] used techniques similar to those employed in deriving the model for the flanged rectangle[7] to develop a model for the airflow into flanged circular hoods. Centerline velocities generated by the model were compared to empirically derived

*Disclaimer: Mention of company names or products does not constitute endorsement by the National Institute for Occupational Safety and Health (NIOSH).

data from a variety of sources, including data generated by Dalla Valle,[2] as a means of testing model validity. Agreement between the theoretical and empirical data varied depending on which data were used but was generally good.

Garrison[9] used a conformal transformation, normally used to obtain the values of the velocity potential for the infinitely long rectangle (AR = 0), to obtain velocity contours for flanged and unflanged circular openings. His solution included the use of Dalla Valle's centerline velocity[2] to calculate some of the parameters in the equation for the velocity potential. Because of the assumptions used in developing the model, it would be considered semi-empirical.

Flynn and Ellenbecker[10] obtained an analytical solution of Laplace's equation in cylindrical coordinates for a flanged circular opening. The solution was not adequate in the vicinity of the hood face. To circumvent this difficulty, Flynn assumed a shape (half oblate ellipsoids) for the equal velocity surfaces based on Dalla Valle's empirical velocities. As will be explained later, the shape and location of the boundary of the flow for most exhaust hood geometries is not known ahead of time. Such an assumption could lead to inaccuracies in the prediction of air velocities.

Esmen et al.[11] applied potential flow theory to derive equations that predict the value of the air velocity at a point in space for single flanged rectangular hoods and for flanged hoods made up of more than one rectangular opening. Their analytical solutions resulted in very cumbersome equations that became more so as boundary surfaces (or baffles) were added to the space under the influence of the hood(s). They did report very good agreement between theoretical and experimental results.

Garrison and Wang[12] used a two-dimensional (2-D) finite element method to solve for the flow into exhaust inlets. They assumed constant velocity at a "distant" flow boundary and a circular shape for that boundary. In comparing the resulting velocity contours to experimental data, they found that the theoretically derived contours overestimate values from the empirically derived data. In a later publication, Garrison and Park[13] compared the experimental velocity contours for plain circular and rectangular exhaust hoods with those generated by the finite element method. The latter tended to overestimate experimental contours also.

Conroy et al.[14] developed a model for a flanged rectangular hood of AR = 0.2 utilizing an existing analytical solution for Laplace's equation for an elliptical aperture with constant potential across the face. The face of the rectangular hood was approximated by both an inscribed ellipse and an ellipse of area equal to that of the face of the rectangle. The analytical solution was found to be limited in describing actual velocity fields. The model was modified by assuming a shape (ellipsoid) for the equal velocity surfaces and assuming that these coincided with the equipotential surfaces. The modified model that used the inscribed ellipse was found to be more accurate in predicting experimental velocity components in the x-direction; the model that used the equal area ellipse was found to be most accurate in predicting z- component velocities. After empirically correcting the former model for z-component velocities, it became an accurate predictor in both directions. In view of the assumptions and adjustments that had to be made, this model may also be considered semi-empirical.

Flynn and Miller[15] used a boundary integral method to solve for the airflow into a flanged rectangular hood of AR = 0.33. They assumed a uniform velocity potential of zero over an imaginary box that constituted the flow boundary and enclosed the hood face. The dimensions of the box were altered until close agreement with the model developed by Tyaglo and Shepelev[7] was achieved. When the authors compared the theoretical and experimental data for the equal velocity contours, good agreement was observed. This would be expected because the model in Reference 7 was used to "calibrate" the model resulting from the boundary integral method. Validation of the boundary integral method should include an independent solution of the problem without using a separate model to determine the shape and location of the boundary.

Anastas and Hughes[16] demonstrated the use of finite difference methods for predicting velocity contours by using a slot configuration with AR = 0.01 or less. This configuration generates essentially 2-D contours. An analytical model was previously derived for the flow field generated by this configuration with conformal mapping techniques. The air velocity contours that were derived by using the numerical method were in excellent agreement with those obtained by using the analytical solution. Experimental centerline and contour data were also in good agreement with theoretically derived air velocities.

A PROPOSED GENERAL APPROACH FOR COMPUTING AIRFLOW FIELDS GENERATED BY EXHAUST HOODS

The previous research discussed above has shown that the assumption of ideal flow leads to accurate prediction of the airflow fields generated by local exhaust hoods of simple geometries. It also has been demonstrated that accurate theoretical prediction of air velocities is possible for flanged hoods of simple geometries because it is possible to accurately calculate the velocity potential at a point in space for these configurations. That is, for flanged hoods it is possible to solve the boundary-value problem by using Laplace's equation because the boundary conditions are known.

For the general case involving plain hoods, configurations with multiple exhaust openings, and other more complex configurations, the boundary conditions are not known a priori. This is the inverse problem of fluid mechanics, in which the boundary's shape and location are obtained as part of the solution. In solving such a problem, one needs to know the governing differential equations and two boundary conditions. The first boundary condition is used to solve the differential equation; the second is used to make appropriate corrections for the location of the boundary. This is the approach taken in solving free-surface flow problems. Allen[17] used this approach in solving for the profile of the free liquid surface for water percolating through a dam wall. The governing differential equation was Laplace's equation in terms of the water pressure, and the two boundary conditions at the free surface were (1) the pressure is zero because it is exposed to the atmosphere and (2) the normal derivative of the pressure is zero because no flow occurs across the boundary surface. A complete solution of the problem

required the use of a third boundary condition, which is derived from the first; namely, that the first derivative of the pressure along the surface is zero. Allen, however, did not provide any quantitative techniques for adjusting the location of the assumed boundary. He only used qualitative criteria related to the direction in which adjustments should be made.

Of interest to designers of local exhaust devices is the ability to predict the air velocities induced at any point in the space under the influence of the device. Air velocity data for exhaust hoods is sometimes presented in the form of a series of equal air velocity surfaces for which the value of the velocity is reported as a percentage of the average velocity across the face of the hood. These surfaces are similar in shape to equipotential surfaces, at least for some configurations. If they were known for the configuration of interest, the flow problem would be considered solved. However, in attempting to solve the flow problem for an arbitrary configuration, one finds that not only are the shapes and locations of the equal velocity surfaces not known, but also the distributions of the velocity potentials along them. That is, the second boundary condition necessary for problem solution is also not known.

It is well known from potential flow theory that for some configurations (such as a point source of suction), the velocity vectors are perpendicular to equipotential surfaces. When this assumption is applied to the general case, the implication is that equipotential surfaces are also equal velocity surfaces. This is true in the general case, provided that the shape of the equipotential surfaces does not change over infinitesimal distances in the direction of the normal to the surfaces. This, however, is not strictly true based on the analysis of data from the model for the plain slot.[16] However, this assumption will be made in what follows in order to explore its usefulness in approximating the flow fields of exhaust hoods in general. A solution utilizing the assumption will consist of the following steps.

1. Specify the value of the constant air velocity contour of interest as a percentage of the average face velocity. Also, assume a constant velocity potential along that contour.
2. Construct a smooth boundary, straddling the hood face, the length of which is obtained from the mass conservation principle based on the airflow through the hood face. The length of the 10% equal air velocity contour for which the velocity value is 10% of the average face velocity would be 10 times the width of the face.
3. Solve Laplace's equation by using a constant potential along the assumed boundary.
4. Calculate the values of the normal derivative along the assumed boundary.
5. Correct the locations of the points along the boundary according to the differences between the specified value of the normal derivative of the potential and those that are calculated.

GOVERNING DIFFERENTIAL EQUATION AND BOUNDARY CONDITIONS

The applicability of the potential flow assumption for flow into local exhaust hoods implies that the flow is incompressible, inviscid, and irrotational. This also means that Laplace's equation, in terms of the velocity potential, ϕ, applies in the space influenced by the local exhaust opening as follows:

$$\partial^2 \phi/\partial x^2 + \partial^2 \phi/\partial y^2 + \partial^2 \phi/\partial z^2 = 0 \quad (1)$$

where x, y, and z are cartesian coordinates.

A slot configuration, which generates a 2-D airflow field, will be used to test the ideas that were advanced in the last section. An analytical model for that configuration may be obtained by conformal transformation. This was explained in the paper by Anastas and Hughes.[16] The relationships between the dimensionless velocity potential, Φ, the stream function, Ψ, and the coordinates X and Y are as follows:

$$X = 1 + \Phi + \exp(\Phi)\cos\Psi \quad (2a)$$

$$Y = \Psi + \exp(\Phi)\sin\Psi \quad (2b)$$

where the above dimensionless variables are defined as

$$\Phi = \phi\,\pi/V_a b,\ \Psi = \psi\,\pi/V_a b,\ X = x\,\pi/b,\ Y = y\,\pi/b$$

For these dimensionless variables, the width of the slot is 2b and the term π arises naturally as a result of the transformation. V_a is the total flow through the hood face divided by the area of the face (or average face velocity) and ψ is the stream function.

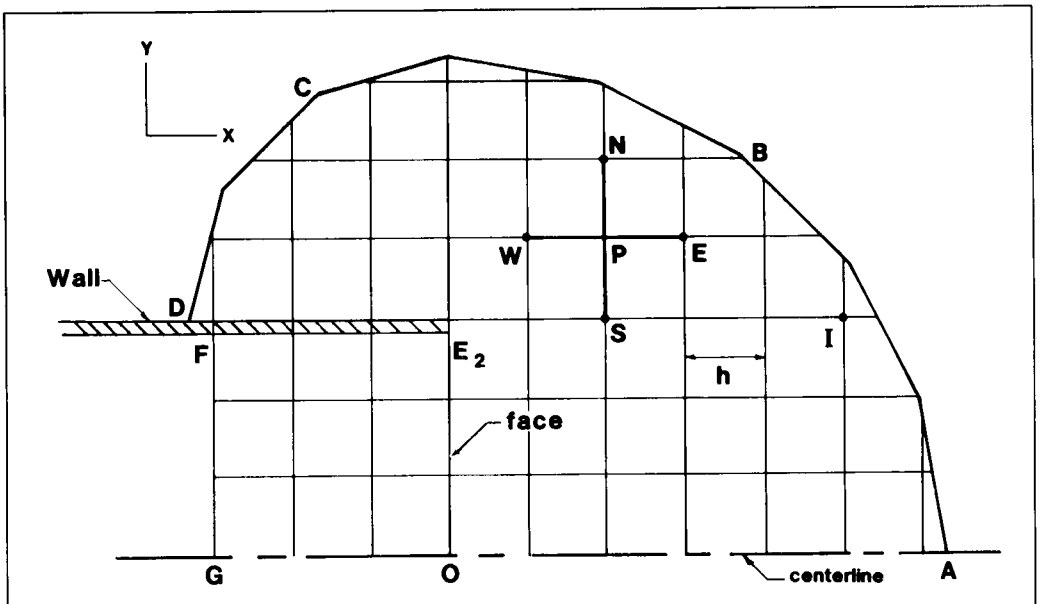

FIGURE 1. Boundary conditions for upper half of a plain slot

Techniques for computing equal velocity contours by using Equations 2a and 2b for the configuration were presented by Anastas and Hughes.[16] Laplace's equation, in terms of the dimensionless variables, becomes

$$\partial^2\Phi/\partial X^2 + \partial^2\Phi/\partial Y^2 = 0 \quad (3)$$

The boundary-value problem for which Equation 3 applies may be solved if either Φ or its normal derivative are specified along the boundary. For the numerical solution of the problem, only one-half of it needs to be solved because of symmetry. The boundary-value problem is shown in Figure 1. A smooth boundary (ABCD) representing the equal velocity contour of interest is laid out on a square grid of size h. The curved boundary is approximated by linear segments, the lengths of which are small multiples of h. Along this boundary, Φ is assumed to be constant and can assume any value because only its derivatives along the boundary are of interest. For a given boundary, the same values of the normal derivatives are obtained along it, no matter what constant value of Φ is assumed. Along the centerline, GOA (Figure 1), the normal derivative, $\partial\Phi/\partial Y$, is zero because of symmetry. It is also zero along DE_2 and FE_2 because there is no flow across the wall of the hood. Well inside the channel part of the flow, the normal derivative along a cross-section (FG) is unity.

SOLUTION OF THE BOUNDARY-VALUE PROBLEM

A finite difference approximation of Equation 3 is the five-point formula that can be used to calculate the potential at an interior Point P, shown in Figure 1, in terms of adjacent points as follows[18]:

$$\Phi_p = (\Phi_N + \Phi_E + \Phi_S + \Phi_W)/4 \quad (4)$$

where N, E, S, and W refer to north, east, south, and west and Φ is dimensionless as before. Equation 4 holds for interior points in the domain $GOABCDE_2F$ shown in Figure 1.

For points along DE_2, but not including Points D and E_2, and for points along GOA but not including A or G, Equation 4 becomes

$$\Phi_{DE_2} \text{ and } \Phi_{GA} = (2\Phi_N + \Phi_E + \Phi_W)/4 \quad (5)$$

because the normal derivative $\partial\Phi/\partial Y$ is zero. For points along E_2F but not including E_2 or F

$$\Phi_{E_2F} = (2\Phi_S + \Phi_E + \Phi_W)/4 \quad (6)$$

The equation for point E_2 is given by

$$\Phi_{E_2} = (2\Phi_E + \Phi_{W1} + \Phi_{W2})/4 \quad (7)$$

where Φ_{W1} and Φ_{W2} are the potentials at points west of E_2 along E_2D and E_2F, respectively.

Along FG, but not including F and G, Equation 4 becomes

$$\Phi_{FG} = (\Phi_N + 2\Phi_E - 2\Delta X + \Phi_S)/4 \quad (8)$$

because the normal derivative is unity along that line. ΔX is equal to the mesh size h in the X direction. A mesh size of $\pi/20$ was found adequate for problem solution.

At Point G:

$$\Phi_G = (2\Phi_N + 2\Phi_E - 2\Delta X)/4 \quad (9)$$

A similar equation may be written for Point F.

For irregular mesh points, such as Point I in Figure 1, finite difference approximations of the second derivatives of Equation 3 may be developed by using a Taylor series expansion, through the second-order term, about Point I.[17] In the X-direction this gives

$$\Phi = \Phi_I + \left(\frac{\partial\Phi}{\partial X}\right)_I (X - X_I) + \frac{1}{2!}\left(\frac{\partial^2\Phi}{\partial X^2}\right)_I (X - X_I)^2 + \ldots \quad (10)$$

With the aid of Figure 2, it can be seen that substitution of $X = X_I - h$ and $X = X_I + hf_1$ in Equation 10 will yield two equations that give the values of the velocity potentials at Points 3 and 1, respectively. Figure 2 shows that f_1 is a fraction of the grid size

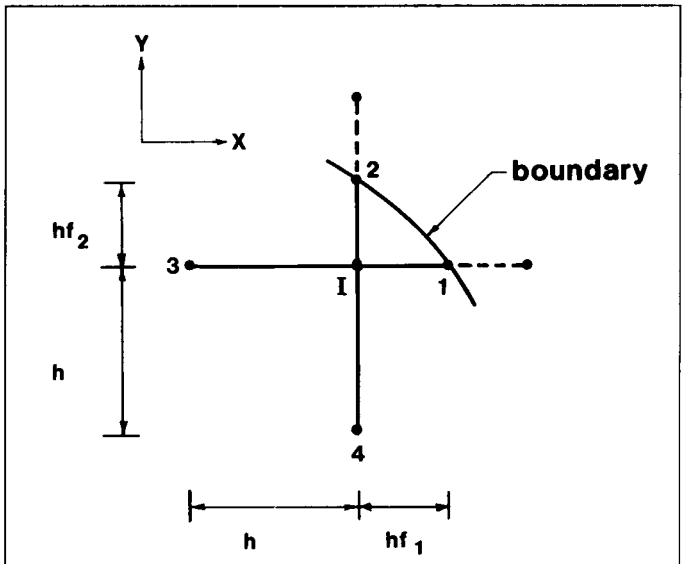

FIGURE 2. Approximation of the velocity potential at an irregular mesh point

h. Elimination of $(\partial\Phi/\partial X)_I$ between the two equations for Points 1 and 3 and solving for $(\partial^2\Phi/\partial X^2)_I$ gives

$$h^2\left(\frac{\partial^2\Phi}{\partial X^2}\right)_I = 2\Phi_1/f_1(1+f_1) - 2\Phi_I/f_1 + 2\Phi_3/(1+f_1) \quad (11)$$

A similar expression may be developed for $h^2(\partial^2\Phi/\partial Y^2)_I$ in terms of f_2. Combining these two terms by using Equation 3 gives

$$\frac{2\Phi_1}{f_1(1+f_1)} + \frac{2\Phi_2}{f_2(1+f_2)} + \frac{2\Phi_3}{(1+f_1)} + \frac{2\Phi_4}{(1+f_2)} - \left(\frac{2}{f_1} + \frac{2}{f_2}\right)\Phi_I = 0 \quad (12)$$

Equation 12 also may be obtained by integrating Equation 3 and by using the mean value theorem for integrals to facilitate the solution as shown by Anderson et al.[19] For irregular mesh points where either f_1 or f_2 are equal to one, the correct expression for Φ_I is obtained by substitution of one into Equation 12 for these quantities. When both are equal to one, Equation 12 reduces to Equation 4, which is applicable to regular mesh points.

Equations 4 through 9 and Equation 12 may be used to write finite difference equations for each point where the velocity

potential is not known. This yields as many simultaneous linear equations as there are unknowns.

Solution of the system of equations was performed by using the Gauss-Seidel method, which utilizes updated values for adjacent points as soon as they are available.[20] Successive over-relaxation (SOR) was used to speed up solution of the system of equations as described by Anastas and Hughes.[16] Convergence was achieved when the sum of the absolute values of the differences between velocity potentials calculated at each mesh point, for two successive iterations, was no greater than 1/100 000.

COMPUTATION OF THE NORMAL DERIVATIVE AT THE BOUNDARY

Once the boundary-value problem has been solved and all values of the velocity potential are known, it is possible to compute the normal derivatives at all irregular mesh points along the boundary. A finite difference expression for the derivative in any direction may be developed by using the Taylor expansion employed in the development of Equation 12. With the aid of Figure 3, it can be seen that the derivative with respect to X at any point may be computed by substituting $X_1 - hf_1$ for Point 2

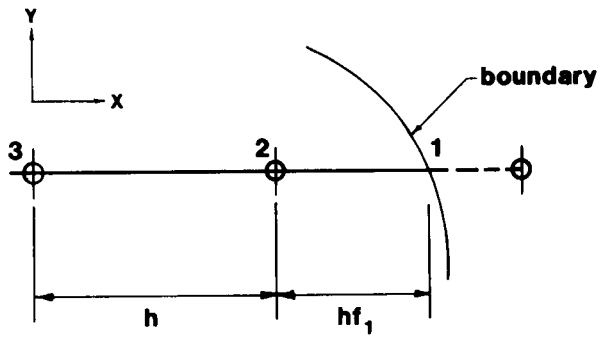

FIGURE 3. Computation of the first derivative at an irregular mesh point

and $X_1 - (1 + f_1)h$ for Point 3 in Equation 10 and solving the resultant two equations for it after elimination of the two terms involving the second derivative. This gives

$$h(\partial\Phi/\partial X)_1 = (1+2f_1)\Phi_1/[f_1(1+f_1)] - (1+f_1)\Phi_2/f_1 + f_1\Phi_3/(1+f_1) \quad (13)$$

Figure 4 shows that Equation 13 also could be used to compute the normal derivative, $\partial\Phi/\partial n$, at Point 1 given the values of the velocity potential at Points 2 and 3 (obtained by interpolation of neighboring points on the grid) and the distances between Points 1 and 2 and Points 2 and 3. The coordinate system (s, n) appearing in Figure 4 consists of the tangent and normal to the boundary at the point.

Because the normal derivative at a point represents the air velocity there, then the surface integral along the boundary is

$$q = \int(\partial\Phi/\partial n)ds \quad (14)$$

which gives the total flow (q) through it. Equation 14 is an important tool in assessing the accuracy of the numerical method

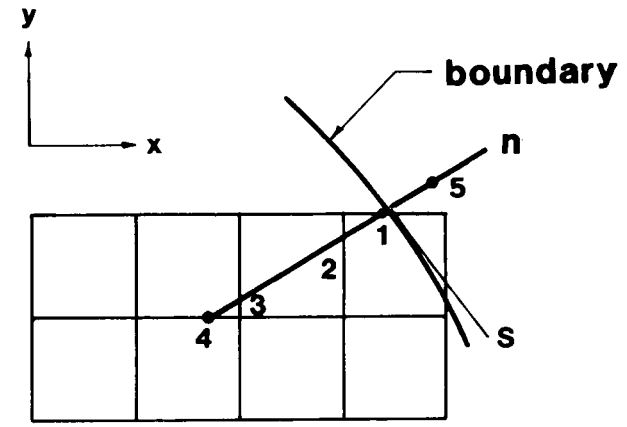

FIGURE 4. Computation of the normal derivative at the boundary

used to solve the boundary-value problem. By performing the integration on a cross-section well inside the channel to the left of the face of the hood, the total flow in the upper half plane is determined to be equal to π. The integral was very close (within 1%) to this value for all boundaries.

ADJUSTMENT OF THE LOCATIONS OF BOUNDARY POINTS

Because the objective of the procedure is the ultimate reduction of the differences between the specified value of the normal derivative and the local values to zero, a suitable numerical technique is required. For this purpose, the Method of False Position was adapted.[20] It is normally used to find the zeros of nonlinear equations involving one variable. Adaptation of the method involved calculation of differences at two locations (Points 1 and 3 in Figure 4) along the normal passing through a point on the boundary. The new location, n_5, is calculated as

$$n_5 = [n_3(\Delta\Phi_\eta)_1 - n_1(\Delta\Phi_\eta)_3]/[(\Delta\Phi_\eta)_1 - (\Delta\Phi_\eta)_3] \quad (15)$$

where $(\Delta\Phi_\eta)_1$ is the difference between the specified value of the normal derivative and the local value at Point 1 and $(\Delta\Phi_\eta)_3$ is the difference at Point 3. An important test for the accuracy for this boundary translation procedure is whether the length of the new boundary equals the length of the old boundary. After all the boundary points have been translated according to Equation 15, the new boundary is smoothed manually by using a french curve. The smoothing can also be performed automatically by using signal processing techniques. The criterion for accepting the numerical procedure should be such that, at all locations in the flow field, the differences between the air velocities calculated from the analytical and numerical models be no more than 1%.

RESULTS AND DISCUSSION

The procedure that was proposed for computing the airflow field generated by the plain slot was applied for the determi-

nation of the 15% velocity contour of that configuration. The initial boundary (Boundary 1 in Figure 5) consisted of two quarter circles, one in each quadrant, with a total length equal to 20.94 units as determined by conservation of mass and from the properties of the flow; namely, that half the width of the slot is equal to 3.1416 and that the normal derivative is equal to 1.0 well inside the channel.[16] As may be noted in Figure 5, the position of the initial boundary is remarkably close to the 15% contour. This boundary was used to generate Boundary 2, shown in Figure 6.

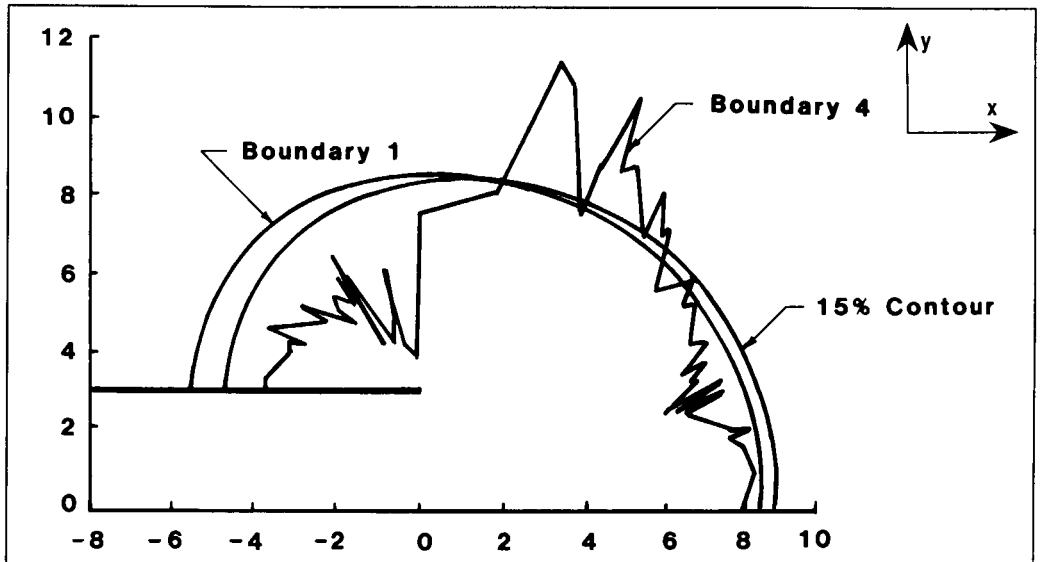

FIGURE 5. Initial and final boundaries for the flow into a slot

The process of generating the boundary produced high-frequency noise, which is typical for such problems, as reported by Haussling and Coleman.[21] The amplitude of the noise was higher for points where the local difference between the specified and calculated normal derivatives was higher.

Equation 15 displaced the initial boundary in the right direction because most values of the normal derivative in the first quadrant were higher than 15% although most of those in the second quadrant were lower. As a result, the boundary points in the first quadrant were displaced in a "northeasterly" direction, along the normal, and those in the second quadrant in a "southeasterly" direction. When compared with the 15% velocity contour, Boundary 2 overshot the "correct" boundary in both quadrants. This, however, does not happen when the Method of False Position is used to solve nonlinear equations in one variable. If the local difference in normal derivatives is negative, it would stay negative until convergence (and vice versa) approaching a zero difference without changing sign. Calculation of the normal derivative for Boundary 2 resulted in values mostly below the specified value in the first quadrant and above that value in the second quadrant, which is exactly the opposite situation for Boundary 1.

Despite this, the procedure for computing the airflow field was continued to see if it does eventually lead to the desired shape and location with the calculated normal derivatives no different from the specified value by more than 1%. After smoothing Boundary 2, the procedure generated Boundary 3 (Figure 7). When compared to the 15% contour, the smoothed version of Boundary 3 nearly coincided with the 15% contour in the second quadrant but was slightly farther out for its first half in the first quadrant and too far in for the second half of it in that quadrant. Calculation of the normal derivatives along Boundary 3 revealed the occurrence of alternating high and low values in its levels along the boundary's entire length. Selected values are reported in Table I. This seemed to indicate a numerical difficulty in solving the differential equation that appears to be related to the shape of Boundary 3. Adjustment of boundary locations by using the data for Boundary 3 led to Boundary 4, shown in Figure 5. Boundary 4 is a worse approximation of the 15% contour than any of the preceding ones.

The Method of False Position usually converges in three or four iterations with every iteration resulting in values closer to the answer. It became clear after inspection of Boundary 4 that

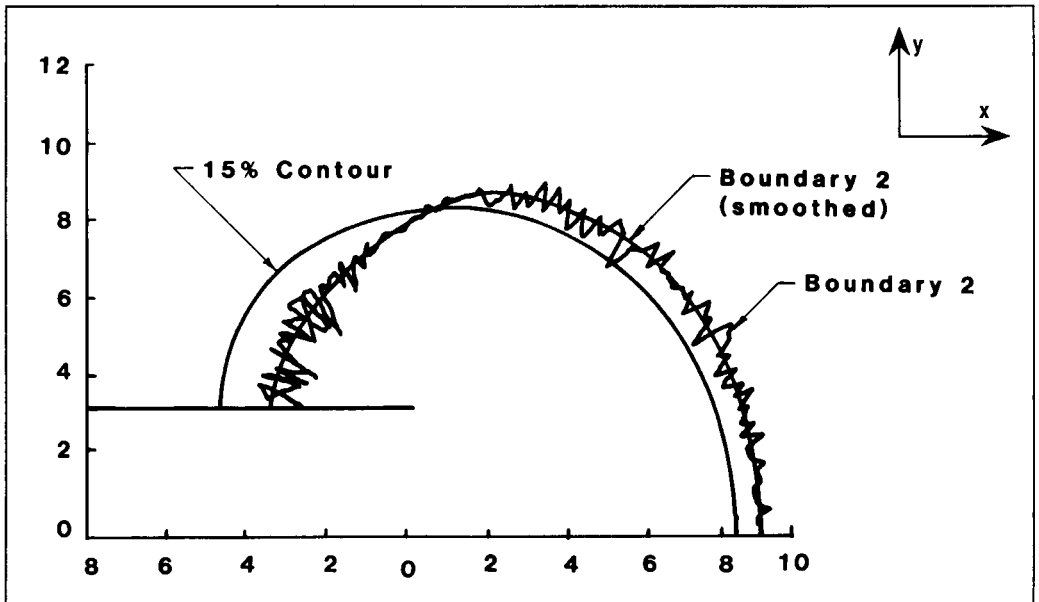

FIGURE 6. Boundary 2 compared to 15% contour

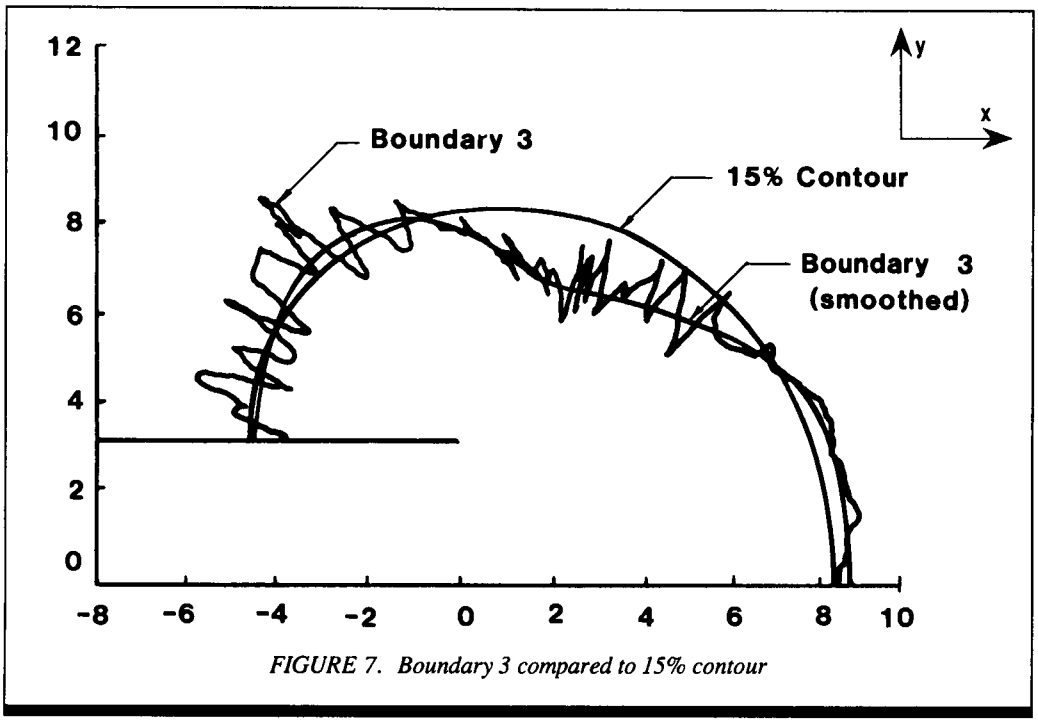

FIGURE 7. Boundary 3 compared to 15% contour

TABLE I. Selected Values of the Normal Derivatives along Boundary 3

X	Y	$\partial\Phi/\partial n$
8.75543	0.15708	0.13088
8.70847	0.62832	0.14246
8.65313	1.09956	0.14419
8.59217	1.57080	0.13768
8.50815	2.04204	0.12891
8.38037	2.51328	0.13712
8.25487	2.98452	0.12787
8.02208	3.61284	0.11113
7.75391	4.08408	0.11496
7.38276	4.56272	0.09456
6.75444	5.00294	0.14791
5.96904	5.50728	0.16577
4.86948	5.99150	0.19795
3.29868	6.50544	0.24186
1.41372	6.99074	0.29628
0.54753	7.53984	0.18397
0.16556	8.01108	0.08435
-0.47124	8.27835	0.06170
-1.57080	8.00565	0.09479
-2.70953	7.53984	0.08407
-3.29868	7.02391	0.0842
-3.61284	6.57235	0.09640
-3.91731	5.96904	0.10696
-4.09378	5.49780	0.11704
-4.24116	4.99803	0.12321
-4.33541	4.55532	0.13100
-4.43458	3.92700	0.13641
-4.51331	3.29868	0.12494

the smoothed version would not provide values of the normal derivative that were within 1% of the specified value. Repetitions of the procedure were, as a result, concluded with Boundary 4.

CONCLUSIONS AND RECOMMENDATIONS FOR FURTHER WORK

The general problem of computing the flow field generated by local exhaust hoods can be considered a boundary-value problem in which the location and shape of the boundary are not known initially but are obtained as part of the solution. In terms of the velocity potential, the flow boundary can be an equipotential surface. However, the second boundary condition (the normal derivative), which is needed to complete solution of the problem, is not available. In order to obtain a solution of the problem in terms of the velocity potential only, it was assumed that an equipotential line is also an equal air velocity contour. Starting with a reasonable initial guess, two other boundaries were generated, and they remained close to the solution. The third boundary, however, diverged from the desired solution. This was, perhaps, because of (1) inaccuracy of the assumption that an equipotential surface is also an equal velocity surface, (2) an insufficiently accurate solution of Laplace's equation for Boundary 3, and (3) a boundary translation algorithm that overcorrects. The theoretical model for the configuration studied (Equations 2a and 2b) suggests that steep gradients in the velocity potential exist at locations of practical significance as is the case for the 15% contour. This renders the solution very sensitive to boundary location.

Three refinements of the above procedure will be proposed. The first involves solving the problem in terms of both the velocity potential and the stream function and performing a correction by using a general relationship between them. The second would involve solving Laplace's equation for these two variables by using the boundary-fitted technique.[21,22] The third would employ a better algorithm for adjusting the location of the boundary.

A solution for the problem may exist in terms of both the velocity potential, Φ, and the stream function, Ψ. In terms of the latter, Equation 3 becomes

$$\partial^2\Psi/\partial X^2 + \partial^2\Psi/\partial Y^2 = 0$$

With the aid of Figure 1, the boundary conditions for the above differential equation are as follows. Along GOA, $\Psi = 0$. The normal derivative, $\partial\Psi/\partial n$, is equal to zero along ABCD and FG. Along both DE_2 and FE_2, $\Psi = \pi$. Adjustment of the boundary location would depend on the relationship $\partial\Psi/\partial s = \partial\Phi/\partial n$, which may be derived from the integral in Equation 14.

In general, it is inadvisable to solve boundary-value problems involving very highly curved surfaces in their physical

domains, as was done in this work for the sake of expediency. For such boundaries and those that are not smooth, numerical problems may arise that could prevent the attainment of a solution. To circumvent these difficulties and to obviate the need for dealing with irregular mesh points (Point I in Figure 1), the boundary-fitted method was developed. Haussling and Coleman[21] used the method to solve for the water wave shape induced by a submerged body moving in shallow water which, again, is a problem in which the boundary is not known initially. More basic details on the method were developed by Thompson et al.[22] In using the technique, the physical domain (Figure 1) is transformed into a rectangle or series of interconnected rectangles by a Laplace equation–type transformation process similar to but more general than the conformal transformation that produced Equations 2a and 2b. This would be called the computational domain, which is used to compute the boundary-fitted coordinates in the physical domain. Finite difference methods are used in generating the grid. Once this is achieved, solution of the differential equation describing the flow is obtained in the computational domain with the appropriate boundary conditions, also transformed, from the physical domain. The desired flow parameters are then mapped onto the physical domain by point-to-point correspondence of the two domains, taking into account the geometry of the boundary in the physical domain.

Finding a substitute for the Method of False Position to translate the boundary locations is difficult because it requires two points to perform a translation and only one is available. In the past, these translations were performed in a qualitative manner by trial-and-error knowing only the direction in which the boundary should be moved.[17] This is feasible provided that a computer is programmed to perform the task. The boundary points could be moved on the screen of a video monitor by using a device similar to a mouse. The software would be capable of reading the new boundary location.

This paper addressed the problem of solving for the air velocities generated by a suction device drawing air from a quiescent medium. This is rarely the case in industrial applications of local exhaust ventilation. Crossdrafts are present there, and they will distort the airflow field calculated for the case where they are absent. A potentially useful method for handling this problem is to impose a velocity field on the one calculated for the quiescent case. The problem then becomes one of velocity vector addition at each point in the space under the influence of the hood. Experimental validation of this approach is necessary because it does not take into consideration air deflected by flanges and other surfaces. This approach was discussed by Dalla Valle,[2] but he offered no experimental validation of the idea. A similar approach would involve the addition of the velocity potentials of both the hood and the crossdraft at a given location and computing the air velocities, in the usual manner, for the resultant flow. This is possible because the velocity potential is a scalar quantity.

ACKNOWLEDGMENT

Many thanks are due Don Murdock for excellent help with the graphics.

REFERENCES

1. **Heinsohn, R.J. and M.S. Choi:** Advanced Design Methods in Industrial Ventilation. In *Ventilation '85*, edited by H.D. Goodfellow. Amsterdam, Holland: Elsevier Science Publishers, 1986.
2. **Dalla Valle, J.M.:** *Exhaust Hoods*. 2d ed. New York: The Industrial Press, 1952.
3. **Silverman, L.:** Centerline Velocity Characteristics of Round Hoods under Suction. *J. Ind. Hyg. Toxicol. 24*:259–266 (1942).
4. **Silverman, L.:** Centerline Velocity Characteristics of Narrow Exhaust Slots. *J. Ind. Hyg. Toxicol. 24*:267–276 (1942).
5. **American Conference of Governmental Industrial Hygienists:** *Industrial Ventilation—A Manual of Recommended Practice*. 19th ed. Cincinnati, Ohio: American Conference of Governmental Industrial Hygienists, 1986. p. 4-4.
6. **Anastas, M.Y. and R.T. Hughes:** Centerline Velocity Models for Flanged Local Exhaust Openings. *Appl. Ind. Hyg. 3(12)*:342–347 (1988).
7. **Tyaglo, I.G. and I.A. Shepelev:** Movement of Airflow to a Suction Opening. *Vodosnabzh. Sanit. Tekh. 5*:24–25 (1970). [Russian].
8. **Drkal, F.:** Theoretical Solution-Flow Conditions for Round Suction Openings with a Flange. *HLH, Z. Heiz., Lueft., Klimatech., Haustech. 21(8)*:271–273 (1970). [German].
9. **Garrison, R.P.:** Velocity Calculation for Local Exhaust Inlet—Graphical Design Concepts. *Am. Ind. Hyg. Assoc. J. 44(12)*:941–947 (1983).
10. **Flynn, M.R. and M.J. Ellenbecker:** The Potential Flow Solution for Air Flow into a Flanged Circular Hood. *Am. Ind. Hyg. Assoc. J. 46(6)*:318–322 (1985).
11. **Esmen, N.A., D.A. Weyel, and F.P. McGuigan:** Aerodynamic Properties of Exhaust Hoods. *Am. Ind. Hyg. Assoc. J. 47(8)*:448–454 (1986).
12. **Garrison, R.P. and Y. Wang:** Finite Element Application for Velocity Characteristics of Local Exhaust Inlets. *Am. Ind. Hyg. Assoc. J. 48(12)*:983–988 (1987).
13. **Garrison, R.P. and C. Park:** Evaluation of Models for Local Exhaust Velocity Characteristics—Part One: Velocity Contours for Freestanding and Bounded Inlets. *Am. Ind. Hyg. Assoc. J. 50(4)*:196–203 (1989).
14. **Conroy, L.M., M.J. Ellenbecker, and M.R. Flynn:** Prediction and Measurement of Velocity into Flanged Slot Hoods. *Am. Ind. Hyg. Assoc. J. 49(5)*:226–234 (1988).
15. **Flynn, M.R. and C.T. Miller:** The Boundary Integral Equation Method (BIEM) for Modeling Local Exhaust Hood Flow Fields. *Am. Ind. Hyg. Assoc. J. 50(5)*:281–288 (1989).
16. **Anastas, M.Y. and R.T. Hughes:** Finite Difference Methods for Computation of Flow into Local Exhaust Hoods. *Am. Ind. Hyg. Assoc. J. 50(10)*:526–534 (1989).
17. **Allen, D.N. deG.:** *Relaxation Methods in Engineering and Science*. New York: McGraw-Hill Book Co., 1954. pp. 203–211.
18. **Ames, W. F.:** *Numerical Methods for Partial Differential Equations*. 2d ed. Orlando, Fla.: Academic Press, 1977. p. 15.
19. **Anderson, D.A., J.C. Tannehill, and R.H. Pletcher:** *Computational Fluid Mechanics and Heat Transfer*. New York: Hemisphere Publishing Corp., 1984. p. 68.
20. **Conte, S.D.:** *Elementary Numerical Analysis*. New York: McGraw-Hill Book Co., 1965. p. 194.
21. **Haussling, H.J. and R.M. Coleman:** "Finite-Difference Computations Using Boundary-Fitted Coordinates for Free-Surface Potential Flows Generated by Submerged Bodies." Proceedings of the Second International Conference on Numerical Ship Hydrodynamics, Berkeley, Calif., 1977. pp. 221–233.
22. **Thompson, J.F., F.C. Thames, and C.W. Mastin:** Automatic Numerical Generation of Body-Fitted Curvilinear Coordinate System for Field Containing Any Number of Arbitrary Two-Dimensional Bodies. *J. Comput. Phys. 15*:299–319 (1974).